



Published in final edited form as:

J Cell Mol Med. 2011 April ; 15(4): 957–969. doi:10.1111/j.1582-4934.2010.01063.x.

DECREASED CAVEOLIN-1 LEVELS CONTRIBUTE TO FIBROSIS AND DEPOSITION OF EXTRACELLULAR IGFBP-5

Yukie Yamaguchi^{*}, Hidekata Yasuoka^{*}, Donna B. Stolz[†], and Carol A. Feghali-Bostwick^{*‡}

^{*} Division of Pulmonary, Allergy, and Critical Care Medicine, University of Pittsburgh School of Medicine, Pittsburgh, Pennsylvania

[‡] Department of Pathology, University of Pittsburgh School of Medicine, Pittsburgh, Pennsylvania

[†] Department of Cell Biology and Physiology, University of Pittsburgh School of Medicine, Pittsburgh, Pennsylvania

Abstract

Our previous studies have demonstrated increased expression of insulin-like growth factor binding protein-5 (IGFBP-5) in fibrotic tissues and IGFBP-5 induction of extracellular matrix (ECM) components. The mechanism resulting in increased IGFBP-5 in the extracellular milieu of fibrotic fibroblasts is unknown. Since Caveolin-1 (Cav-1) has been implicated to play a role in membrane trafficking and signal transduction in tissue fibrosis, we examined the effect of Cav-1 on IGFBP-5 internalization, trafficking, and secretion. We demonstrated that IGFBP-5 localized to lipid rafts in human lung fibroblasts and bound Cav-1. Cav-1 was detected in the nucleus in IGFBP-5-expressing fibroblasts, within aggregates enriched with IGFBP-5, suggesting a coordinate trafficking of IGFBP-5 and Cav-1 from the plasma membrane to the nucleus. This trafficking was dependent on Cav-1 as fibroblasts from Cav-1 null mice had increased extracellular IGFBP-5, and as fibroblasts in which Cav-1 was silenced or lipid raft structure was disrupted through cholesterol depletion also had defective IGFBP-5 internalization. Restoration of Cav-1 function through administration of Cav-1 scaffolding peptide dramatically increased IGFBP-5 uptake. Finally, we demonstrated that IGFBP-5 in the ECM protects fibronectin from proteolytic degradation. Taken together, our findings identify a novel role for Cav-1 in the internalization and nuclear trafficking of IGFBP-5. Decreased Cav-1 expression in fibrotic diseases likely leads to increased deposition of IGFBP-5 in the ECM with subsequent reduction in ECM degradation, thus identifying a mechanism by which reduced Cav-1 and increased IGFBP-5 concomitantly contribute to the perpetuation of fibrosis.

Keywords

Caveolin-1; insulin-like growth factor binding protein-5; fibrosis; extracellular matrix

INTRODUCTION

Fibrotic disorders, including systemic sclerosis (SSc) and idiopathic pulmonary fibrosis (IPF), are characterized by excessive deposition of extracellular matrix (ECM) components such as collagen and fibronectin [1,2]. Fibrosis is the result of abnormal ECM remodeling which occurs due to an imbalance of ECM deposition and degradation [3,4]. Activated

fibroblasts are a primary source of ECM in fibrotic tissues [5]. Although numerous studies have explored the fibrotic process in different tissues, the exact pathogenic mechanism responsible for fibrosis in SSc and IPF has not been elucidated.

Caveolin-1 (Cav-1) is a 22-kDa membrane protein essential for the formation of flask-shaped 50–100 nm membrane invaginations termed caveolae [6]. Since caveolae have a distinctive composition of lipids, including cholesterol and sphingolipids, they serve as a platform for processes such as trafficking, endocytosis, and signaling [7–9]. Cav-1 was recently implicated in fibrosis. Kasper *et al* first reported abnormal Cav-1 expression in type I pneumocytes during lung fibrogenesis [10]. Tourkina *et al* subsequently identified a role for Cav-1 in regulating collagen expression in lung fibroblasts [11]. In addition, markedly decreased expression of Cav-1 in primary fibroblasts, lung and skin tissues of patients with SSc and IPF was reported [12,13]. Several studies have shown that Cav-1 regulates a variety of signaling molecules and receptors, including Smad/TGF- β receptor, Akt, ERK1/2, and MEK, which interact with caveolin-1 scaffolding domain corresponding to amino acids 82-101 of Cav-1 [14–16]. Further confirmation for the role of Cav-1 in fibrosis was demonstrated in Cav-1 knockout mice, which exhibit a wide range of fibrosis-like lung abnormalities including thickening of lung alveolar septa and presence of hypertrophic type II pneumocytes [17,18].

Insulin-like growth factor binding proteins (IGFBPs) were originally reported as regulators of Insulin-like growth factor (IGF)-I function [19]. Secreted IGFBPs serve as carriers of IGF-I and modulate IGF-I actions, either potentiating or inhibiting them. Several studies have reported that IGFBPs also exert IGF-I-independent effects [20–23]. IGFBP-3 and -5 are the most abundant and conserved IGFBPs, respectively. They are secreted proteins which can also translocate to the nucleus via a nuclear localization sequence [24,25]. Nuclear IGFBP-3 and -5 are believed to be derived from the corresponding secreted proteins, and their uptake by cells likely occurs through putative receptors which have not yet been identified[26].

We have previously reported that IGFBP-5 is significantly increased in dermal and pulmonary fibroblasts and tissues of patients with SSc and IPF [27,28]. IGFBP-5 binds ECM components and its deposition in the extracellular milieu is increased in fibrotic cells and tissues [28]. Notably, IGFBP-5 induces the production of ECM components *in vitro* by IGF-I independent mechanisms [29,30] and triggers a fibrotic phenotype *in vivo*[31] that includes induction of ECM production, myofibroblastic transformation and infiltration of mononuclear cells [29,32]. Furthermore, IGFBP-5 triggers significant fibrosis in human skin using an *ex vivo* organ culture model [33].

In this study, we investigated the internalization and nuclear translocation of IGFBP-5 in association with Cav-1 in primary lung fibroblasts. Our findings demonstrate that IGFBP-5 binds Cav-1, is internalized via Cav-1-mediated pathways, and subsequently translocates to the nucleus as vesicular-like aggregates that lack a membrane and contain Cav-1. Further, IGFBP-5 is increased in the ECM of fibroblasts from Cav-1 null mice and likely protects ECM components from degradation. Thus, in fibrotic disorders such as SSc and IPF, reduced Cav-1 levels result in increased extracellular levels of IGFBP-5, which then contributes to fibrosis both by inducing ECM production and protecting ECM components from degradation.

MATERIALS AND METHODS

Primary fibroblast culture

Human primary lung fibroblasts were cultured under a protocol approved by the University of Pittsburgh Institutional Review Board from the explanted lungs of normal organ donors. Mouse primary lung fibroblasts were cultured from lung tissues of C57BL/6J WT mice and Cav-1 null mice (Cav-1^{-/-}) (The Jackson Laboratory, Bar Harbor, ME). Approximately 2-cm pieces of peripheral lung were minced and fibroblasts were cultured in Dulbecco's modified Eagle's medium (DMEM; Mediatech, Herndon, VA) supplemented with 10% FBS, penicillin, streptomycin, and anti-mycotic agent, as previously described [27].

Adenovirus Construct Preparation

Adenovirus constructs were generated as previously reported [28]. Briefly, the full-length cDNAs of human IGFBP-3 and -5 were obtained by RT-PCR using total RNA extracted from primary human fibroblasts. The cDNAs were subcloned into the shuttle vector pAdlox and used for the preparation of replication-deficient adenovirus serotype 5 expressing IGFBP-3 (Ad3), IGFBP-5 (Ad5), 3xFLAG-tagged IGFBP-5 (Ad5-FLAG) or, as a control, no cDNA (cAd) in the Vector Core Facility at the University of Pittsburgh. Replication-deficient adenovirus serotype 5 expressing mouse early growth response (Egr)-1 (AdEgr-1) was generously provided by Dr. John Varga (Northwestern University, Chicago, IL). Human and mouse primary lung fibroblasts were infected with adenovirus at a multiplicity of infection (MOI) of 50. In some experiments, supernatant from 3XFLAG-IGFBP-5-expressing fibroblasts (FLBP-5) was added to fibroblasts in culture. Briefly, fibroblasts were thoroughly rinsed with 1xPBS following infection with Ad5-FLAG and cultured in fresh media. After 24h, supernatants were harvested and centrifuged for 10 minutes to pellet cell debris.

Purification of Caveolae-enriched membrane fractions

Caveolae-enriched membrane fractions were purified as previously described [34]. Briefly, human lung fibroblasts were plated on 100 mm dishes and cultured for 48h untreated or following infection with cAd or Ad5. Cells were homogenized in Triton-MBS buffer (25 mM MES, 150 mM NaCl, pH 6.5, 1% Triton X-100), adjusted to 40% sucrose by the addition of an equal volume of 80% sucrose, and overlaid with a 5–35% discontinuous sucrose gradient. The samples were centrifuged at 39,000 rpm for 18h in an SW41 rotor (Beckman Instruments, Palo Alto, CA). Twelve fractions were collected and subjected to western blot analysis.

Immunoprecipitation

1.2×10^6 fibroblasts were cultured on 100mm dishes and were either untreated or infected with cAd or Ad5 for 72 hours and scraped in 350 μ l RIPA buffer (50 mM Tris-HCl pH 8.0, 150 mM NaCl, 1% NP-40, 0.5% sodium deoxycholate) containing protease inhibitor cocktail (Sigma-Aldrich, St. Louis, MO). Lysates were incubated with 2 μ g Caveolin-1 antibody (Santa Cruz Biotechnology, Santa Cruz, CA) or control IgG at 4°C. A mixture of agarose beads conjugated with Protein A and Protein G (Invitrogen Life Technologies, Carlsbad, CA) were added for an additional 4 hours. Bound complexes were washed with RIPA buffer and resuspended in 50 μ l 2x sodium dodecyl sulfate (SDS) gel-loading buffer (125mM Tris HCl, pH 6.8, 10% glycerol, 2% SDS, 715 mM mercaptoethanol, 0.003% bromophenol blue) for western blot analysis.

Transmission electron microscopy

Cells grown on tissue culture plastic were fixed in 2.5% glutaraldehyde in 100 mM PBS (8 gm/l NaCl, 0.2 gm/l KCl, 1.15 gm/l Na₂HPO₄·7H₂O, 0.2 gm/l KH₂PO₄, pH 7.4) for 1 hr at 4°C. Monolayers were washed in PBS three times and post-fixed in aqueous 1% osmium tetroxide, 1% Fe₆CN₃ for 1 hr. Cells were washed 3 times in PBS then dehydrated through a 30–100% ethanol series followed by several changes of Polybed 812 embedding resin (Polysciences, Warrington, PA). Cultures were embedded by inverting Polybed 812-filled BEEM capsules on top of the cells. Blocks were cured overnight at 37°C, and then cured for two days at 65°C. Monolayers were pulled off the coverslips and re-embedded for cross sectioning. Ultrathin cross sections (60 nm) of the cells were obtained on a Riechart Ultracut E microtome, post-stained in 4% uranyl acetate for 10 min and 1% lead citrate for 7 min. Sections were viewed on a JEOL JEM 1011 transmission electron microscope (JEOL, Peabody MA) at 80 KV.

Immunoelectron Microscopy

Cells were fixed in cryofix (2% paraformaldehyde, 0.01% glutaraldehyde in 0.1 M PBS) and stored at 4°C for 1 hour. Cells were pelleted and resuspended in a small amount of 3% gelatin in PBS, solidified at 4°C, then fixed an additional 15 min in cryofix. Gelatin-cell block was cryoprotected in PVP cryoprotectant overnight at 4°C (25% polyvinylpyrrolidone, 2.3 M sucrose, 0.055M Na₂CO₃, pH 7.4) as described previously [35]. Cell blocks were frozen on ultracryotome stubs under liquid nitrogen and stored in liquid nitrogen until use. Ultrathin sections (70–100nm) were cut using a Reichert Ultracut U ultramicrotome with a FC4S cryo-attachment, lifted on a small drop of 2.3 M sucrose and mounted on Formvar-coated copper grids. Sections were washed three times with PBS, then three times with PBS containing 0.5% bovine serum albumin and 0.15% glycine (PBG buffer), followed by a 30 min blocking incubation with 5% normal goat serum in PBG. Sections were labeled with anti-Caveolin-1 (BD transduction Laboratories, Lexington, KY) and anti-IGFBP-5 (Gropep Ltd, Adelaide, Australia) antibodies. Sections were washed four times in PBG and labeled with goat anti-rabbit (5 nm) or goat anti-mouse (10 nm) gold conjugated secondary antibodies (Amersham Biosciences, Piscataway, NJ), each at a dilution of 1:25 for 1 hr. Sections were washed three times in PBG, three times in PBS, then fixed in 2.5% glutaraldehyde in PBS for 5 min, washed two times in PBS and six times in ddH₂O. Sections were post-stained in 2% neutral uranyl acetate, for 7 min, washed three times in ddH₂O, stained 2 min in 4% uranyl acetate, then embedded in 1.25% methyl cellulose. Labeling was observed on a JEOL JEM 1210 electron microscope (Peabody, MA) at 80 kV.

Western blot analysis

Supernatants, cellular lysates, and ECM were obtained from cultured fibroblasts as previously described [28] with some modifications. Briefly, 2.0×10^5 primary fibroblasts were cultured in 35-mm wells. Lysates were harvested using RIPA buffer containing protease inhibitor cocktail. Cellular supernatants and lysates were resuspended in 6xSDS gel-loading buffer. ECM was scraped directly in 200µl 2xSDS gel-loading buffer as previously described[28]. All samples were analyzed by western blot using one of following antibodies: anti-IGFBP-3, anti-Caveolin-1, anti-Egr-1, anti-fibronectin, anti-type I collagen α 1 chain, anti-GAPDH (Santa Cruz Biotechnology), anti-human IGFBP-5 (Gropep Ltd), anti-mouse IGFBP-5 (UBI, Lake Placid, NY), anti-alpha tubulin, anti-58k Golgi protein (Abcam Inc, Cambridge, MA), anti-FLAG M2 (Sigma-Aldrich), anti-Histone H3 (Cell Signaling, Beverly, MA), and anti-vitronectin (Bio genesis, Mill Creek, WA). Signals were detected following incubation with horseradish peroxidase-conjugated secondary antibody and chemiluminescence (Perkin Elmer Life Sciences, Inc., Boston, MA).

Preparation of fibroblast nuclear and cytoplasmic extracts

Nuclear and cytoplasmic fractions were extracted from cultured human and mouse fibroblasts as previously described[36]. Briefly, 1×10^6 fibroblasts were cultured in 100 mm dishes and scraped with 400 μ l of Buffer A (10 mM HEPES-KOH pH 7.9, 1.5 mM MgCl₂, 10 mM KCl, 0.5 mM dithiothreitol, 0.2 mM PMSF). Lysates were incubated on ice for 10 minutes. After centrifugation at 12000 rpm for 30 seconds, supernatant (cytoplasmic extract) was harvested. The pellet was washed 3 times using 400 μ l buffer A to remove any residual cytoplasmic extracts and resuspended in 100 μ l Buffer C (20 mM HEPES-KOH pH7.9, 25% glycerol, 420 mM NaCl, 1.5 mM MgCl₂, 0.2 mM EDTA, 0.5mM DTT, 0.2mM PMSF) on ice for 20 minutes with intermittent vortexing. After centrifugation at 12000 rpm for 30 seconds, supernatant (nuclear extract) was harvested. Nuclear and cytoplasmic extracts were stored at -80°C , and used for western blot analysis.

Immunocyto staining

Human or mouse fibroblasts were cultured on cover slips coated with type I collagen (BD Biosciences, Belford, MA). After infection with adenoviral constructs for 48h, cells were fixed for 20 min in PBS containing 2% paraformaldehyde or methanol and acetone (1:1), and permeabilized with 0.1% Triton X-100 for 15 min. Cover slips were blocked with 5% serum for 1h, and incubated with anti-IGFBP-5 (Groppe Ltd) or anti-Cav-1 (BD Transduction Laboratories) antibodies followed by Alexa Flour[®] 488- or 555-conjugated donkey anti-mouse- or rabbit-IgG antibodies (Invitrogen). Appropriate IgG was used as a control antibody. Hoechst (Sigma-Aldrich) was used to identify nuclei. Images were taken on an Olympus Fluoview 1000 microscope (Olympus America Inc., Melville, NY) using identical camera settings.

IGFBP-5 degradation assay

2.0×10^5 WT and Cav-1^{-/-} lung fibroblasts were seeded in 35-mm wells and cultured in serum-free medium for 24h. Conditioned media were harvested and centrifuged to remove cell debris. Supernatants were mixed with recombinant IGFBP-5 protein (rBP5; final concentration 500 ng/ml), and incubated at 37 $^{\circ}\text{C}$ for 1h. 6xSDS gel-loading buffer was added, and samples were subjected to western blot analysis for the detection of IGFBP-5.

Detection of IGFBP-5 mRNA

IGFBP-5 and β -actin mRNA expression in cultured fibroblasts was examined using RT-PCR. Total RNA from WT and Cav-1^{-/-} fibroblasts was extracted using TRIzol[®]. First-strand cDNA was synthesized using random primers and Superscript[™] II reverse transcriptase (Invitrogen). IGFBP-5 and β -actin mRNAs were detected by PCR using cDNA (50 ng total RNA equivalent) as a template. Primer sets were forward: 5'-GAGGTGGTGACAGAGCAGGT-3', reverse: 5'-TCTCGGAGTCTGGCTTTACC-3' to amplify mouse IGFBP-5 (600 bp), and forward: 5'-ATGTTTGAGACCTTCAACAC-3', reverse: 5'-CACGTCACTTCATGATGG-3' to amplify β -actin (494 bp). PCR products were separated by electrophoresis on 1 % agarose gels and stained with ethidium bromide.

Disruption of caveolar structure

To disrupt caveolae, Methyl- β -cyclodextrin (M β CD; Sigma-Aldrich) was used. Briefly, primary lung fibroblasts were incubated in the presence or absence of 10mM M β CD for 1h at 37 $^{\circ}\text{C}$ under serum-free conditions.

Silencing of Cav-1

Caveolin-1-specific small interfering RNA (siRNA) was purchased from Applied Biosystems/Ambion (Austin, TX). Scrambled siRNA was used as negative control. $2.0 \times$

10⁵ primary fibroblasts were seeded in 35-mm wells supplemented with DMEM containing 10% FBS but no antibiotics. Cells were transfected with 100 pmol siRNA using Lipofectamine 2000 (Invitrogen) and cultured for 48 hours prior to harvesting.

Treatment with Cav-1 scaffolding peptide

A peptide corresponding to the Cav-1 scaffolding domain (CSD: amino acids 82-101 of Cav-1; DGIWKASFTTFTVTKYWFYR) and a scrambled control peptide (Cont: WGIDKAFFTTSTVTYKWFYR), carrying the antennapedia internalization sequence (RQIKIWFQNRRMKWKK), were purchased from Calbiochem (San Diego, CA). Human lung fibroblasts at 70–80% confluence were cultured for 16 hr in serum-free DMEM then treated with 5 μM CSD or Control peptide as previously described [16] for 1h. Cells were harvested and used for immunoblotting.

ECM degradation assay

Cell culture wells were coated with human fibronectin (FN; Sigma-Aldrich) at 1 μg/cm². Human recombinant IGFBP-5 (Groppe Ltd) or vehicle (10mM HCl) was added to the wells and incubated at 4°C for 16 hr to allow IGFBP-5 to bind FN. The wells were washed with 1xPBS prior to the addition of media conditioned by the culture of normal fibroblasts. Conditioned media were mixed with or without the following protease inhibitors: 10mM PMSF, 10mM EDTA, and protease inhibitor cocktail (PI; Sigma-Aldrich), agitated on a shaker for 6 hr at 37 °C, then added to the wells for 48h incubation. ECM was harvested and used for immunoblotting.

Statistical Analysis

Statistical comparisons were performed using the paired or unpaired Student-*t* test as appropriate.

RESULTS

IGFBP-5 localizes to Caveolin-1-enriched fractions and binds to Caveolin-1

We first examined whether IGFBP-5 localized to Caveolin-enriched fractions in untreated and IGFBP-5-expressing fibroblasts. As shown in Figure 1A, IGFBP-5 was detected in Cav-1 containing cellular fractions (fractions 4–6). IGFBP-5 levels in these fractions were more modest in untreated compared to IGFBP-5-expressing fibroblasts, indicating that IGFBP-5 and Cav-1 co-localize in lipid rafts. To determine whether IGFBP-5 binds Cav-1 in human fibroblasts, co-precipitation assays were used. As shown in Figure 1B, IGFBP-5 co-precipitated with Cav-1 in both untreated (left panel) and IGFBP-5 expressing (right panel) fibroblasts, demonstrating that IGFBP-5 and Cav-1 form protein complexes at baseline and under high IGFBP-5 expression conditions.

Caveolin-1 translocates to the nucleus in IGFBP-5-expressing fibroblasts

Since IGFBP-5 is a secreted protein that translocates to the nucleus to exert its transcription-regulatory activity[20], we hypothesized that the interaction of Cav-1 with IGFBP-5 on the cell membrane may result in nuclear trafficking of both proteins. We therefore examined Cav-1 levels in nuclear extracts of IGFBP-5-expressing primary fibroblasts. As shown in figure 2A, the relative distribution of Cav-1 in cytoplasmic and nuclear fractions of non-treated (left panel) and cAd-treated (right panel) primary fibroblasts was comparable. In contrast, Cav-1 levels were 40% greater in nuclear extracts of IGFBP-5-expressing fibroblasts (Figure 2A, right panel). The nuclear localization of Cav-1 was further confirmed using immunofluorescence. Immunocytostaining of Cav-1 and IGFBP-5 revealed the presence of Cav-1 in the nuclei of IGFBP-5-expressing fibroblasts (Figure 2B). Since Jurgeit

et al had reported that IGFBP-5 is present in intracellular vesicles outside the nucleus [37], we extended our confirmation of Cav-1 and IGFBP-5 co-localization and nuclear translocation using electron microscopy (Figure 3). Vesicle-like structures were detected in the cytoplasm and the nucleus of IGFBP-5 expressing fibroblasts (Figure 3B–F) but were not present in control fibroblasts (Figure 3A). Extensive analysis of the vesicle-like structures revealed the absence of a membrane, suggesting that they consisted of protein aggregates. Upon entry in the nucleus, aggregates of various sizes seemed to fuse and form larger and denser aggregates (Figure 3C–F). Using immunoelectron microscopy, we confirmed that both Cav-1 and IGFBP-5 are components of these aggregates in IGFBP-5-expressing fibroblasts (Figure 3G–L).

IGFBP-5 compartmentalization is altered in cytoplasmic and nuclear extracts purified from Caveolin-1 deficient fibroblasts

We next sought to determine whether Cav-1 is required for IGFBP-5 nuclear translocation. Levels of IGFBP-5 were compared in cytoplasmic and nuclear extracts from IGFBP-5-expressing WT and Cav-1^{-/-} fibroblasts. As shown in Figure 4C and 4F, compared to WT fibroblasts, Cav-1^{-/-} fibroblasts had significantly lower levels of IGFBP-5 in both the nucleus and cytoplasm. Similar results were observed for IGFBP-3 in Cav-1^{-/-} fibroblasts infected with Ad3 (Figure 4D & F). To exclude the possibility that Cav-1 deficiency prevents efficient adenoviral infection, we infected the fibroblasts with an adenovirus expressing human Egr-1, a transcription factor known to localize to the nucleus[38]. Egr-1 levels were comparable in nuclear extracts from WT and Cav-1^{-/-} fibroblasts (Figure 4E & F), suggesting that reduced IGFBP nuclear translocation in Cav-1 null fibroblasts is not due to hindrance of adenoviral infection and that nuclear compartmentalization of IGFBP-3 and IGFBP-5 requires Caveolin-1.

Absence of Caveolin-1 is associated with low intracellular and high extracellular levels of IGFBP-5

Having observed a lack of IGFBP-5 in the cytoplasmic and nuclear fractions of IGFBP-5-expressing Cav-1^{-/-} fibroblasts, we compared intracellular IGFBP-5 levels to those secreted and deposited in the ECM. As shown in Figure 5A, IGFBP-5 levels were significantly reduced in lysates of Cav-1^{-/-} fibroblasts. This was further confirmed using immunocytochemistry (Figure 5B). In contrast to cellular lysates, IGFBP-5 levels in the extracellular milieu in both media conditioned by IGFBP-5 expressing Cav-1^{-/-} fibroblasts and the ECM deposited by the cells were higher than those in their WT counterparts (Figure 5C). IGFBP-5 can be proteolytically cleaved by several different proteases, and increased extracellular levels of IGFBP-5 can result from reduced IGFBP-5 degradation. To compare IGFBP-5 degradation in WT and Cav-1^{-/-} fibroblasts, we used a degradation assay. As shown in Figure 5D, levels of intact rBP5 were comparable in the presence of media conditioned by WT and Cav-1^{-/-}, indicating that the absence of Cav-1 does not modulate the extracellular degradation of IGFBP-5. To further evaluate the effects of Cav-1 on IGFBP-5 expression, we examined steady-state mRNA levels of IGFBP-5 in WT and Cav-1^{-/-} fibroblasts. At baseline, Cav-1^{-/-} lung fibroblasts had significantly higher IGFBP-5 mRNA levels compared to WT cells (Figure 5E), likely a compensatory response to the reduced intracellular protein levels of IGFBP-5 in Cav-1^{-/-} fibroblasts.

Caveolin-1 regulates nuclear compartmentalization of IGFBP-5

Increased levels of extracellular IGFBP-5 and decreased intracellular levels in Cav-1^{-/-} mouse fibroblasts led us to speculate that Cav-1 might regulate the internalization of secreted IGFBP-5. To determine if secreted IGFBP-5 requires Cav-1 for internalization, 3xFLAG-tagged IGFBP-5 (FLBP-5) secreted by WT fibroblasts was added to WT and Cav-1^{-/-} fibroblasts. After 15 minutes, IGFBP-5 levels corresponding to internalized

protein were detected in cellular lysates using anti-FLAG antibody. As shown in Figure 6A, Cav-1^{-/-} fibroblasts had lower intracellular IGFBP-5 levels compared with WT fibroblasts, indicating that Cav-1 facilitates IGFBP-5's internalization. To differentiate caveolin-containing caveolae from lipid rafts, we disrupted fibroblast lipid rafts with M β CD. To reduce Cav-1 levels and emulate those in fibrotic disease, we also silenced Cav-1 expression using sequence-specific siRNA. Silencing Cav-1 resulted in a 52% reduction in corresponding protein levels. Purified 3xFLAG-tagged IGFBP-5 was then added to these fibroblasts, and lysates were harvested after 5, 15, and 30 minutes. Tagged IGFBP-5 was detected using anti-FLAG antibody. Whereas uptake of tagged IGFBP-5 increased in a time-dependent manner in control fibroblasts, lower levels of IGFBP-5 were observed in lysates of fibroblasts treated with M β CD and those in which Cav-1 was silenced 15 and 30 minutes following the addition of FLAG-tagged IGFBP-5 (Figure 6B, C). The decrease in IGFBP-5 uptake reached significance at 30 minutes (Figure 6B & C, right panels). Depletion of cholesterol and silencing of Cav-1 both reduced cellular uptake of IGFBP-5, suggesting that both Cav-1 and intact caveolae contribute to the internalization of IGFBP-5.

IGFBP-5 trafficking can be restored by restitution of Cav-1 function

The Cav-1 CSD peptide can bind to a variety of proteins, and restoration of Cav-1 function can be accomplished by delivery of Cav-1 CSD [39]. We used a cell-permeable Cav-1 CSD peptide at concentrations shown by others to restore Cav-1 function [12,16], to evaluate whether restoration of Cav-1 function facilitates normal uptake of IGFBP-5. Briefly, Cav-1^{-/-} fibroblasts were treated with 5 μ M Cav-1 CSD peptide for 1h, and then purified FLAG-tagged IGFBP-5 was added. Fibroblasts were harvested and IGFBP-5 levels were detected by immunoblotting. As shown in Figure 7, restoration of Cav-1 function in Cav-1^{-/-} fibroblasts using Cav-1 CSD peptide dramatically increased IGFBP-5 internalization, thus restoring IGFBP-5 trafficking.

IGFBP-5 protects ECM components from degradation

We have previously demonstrated increased expression, secretion, and ECM deposition of IGFBP-5 in primary fibroblasts from patients with SSc and IPF [27,28]. We have also reported that IGFBP-5 induces production of collagen and fibronectin and binds these ECM components [28]. In addition, we and others have reported reduced levels of Cav-1 in primary fibroblasts from patients with SSc and IPF [12,13]. In view of these findings, we speculated that increased IGFBP-5 deposition in the ECM of fibrotic cells resulted from impairment of IGFBP-5 cellular entry due to low expression of Cav-1. We therefore explored the possibility that in cells with reduced Cav-1 levels, IGFBP-5 deposited in the ECM could protect ECM components from degradation, thus contributing to the fibrotic phenotype. Human rBP5 was added to fibronectin (FN)-coated plates and allowed to bind overnight. Media conditioned by fibroblasts, presumed to be a source of proteases that can degrade ECM components, was added to the IGFBP-5-bound FN in the presence or absence of protease inhibitors. After 48h, ECM was harvested and FN levels were examined by immunoblotting using an antibody that recognizes the EDA-containing domain specific to matrix FN. As shown in Figure 8, FN levels in rBP5-bound FN-coated wells were notably higher than those in vehicle treated FN-coated wells, confirming our previous observations [28] and establishing that IGFBP-5 can bind to FN and afford it protection from proteolytic activity. In the presence of conditioned media supplemented with PMSF and protease inhibitor cocktail-, but not EDTA-treated supernatants, FN levels in the ECM were higher, suggesting that FN was protected from degradation. Although degraded FN fragments could not be detected using the FN antibody, taken together, our results indicate that IGFBP-5-bound FN in ECM is protected from proteolytic degradation.

DISCUSSION

Our goal was to evaluate the association of Cav-1 and IGFBP-5 and the role of Cav-1 in IGFBP-5 internalization in lung fibroblasts and thus elucidate the pathogenic mechanism mediating fibrosis as a result of reduced Cav-1 expression. In primary fibroblasts, IGFBP-5 bound Cav-1, and both proteins translocated to the nucleus in IGFBP-5-expressing fibroblasts. Electron microscopy revealed the presence of IGFBP-5 and Cav-1 within aggregates in the nucleus. Caveolar disruption and Cav-1 silencing inhibited IGFBP-5 internalization. Conversely, restoration of Cav-1 function using Cav-1 CSD peptide facilitated cellular uptake of IGFBP-5 in Cav-1^{-/-} fibroblasts. Accumulation of secreted IGFBP-5 in the ECM of Cav-1^{-/-} fibroblasts increased as intracellular levels decreased. Steady-state mRNA levels of mouse IGFBP-5 increased in Cav-1^{-/-} fibroblasts, probably reflecting a compensatory mechanism in response to reduced intracellular levels of IGFBP-5 protein. Unlike mRNA levels, the degradation of IGFBP-5 in the extracellular milieu was similar in WT and Cav-1^{-/-} fibroblasts, suggesting that inhibition of proteolytic cleavage does not explain the increased extracellular deposition of IGFBP-5 in the absence of Cav-1.

In primary pulmonary fibroblasts, IGFBP-5 co-localized with Cav-1 and both proteins formed complexes. In addition, Cav-1 CSD peptide significantly increased the intracellular uptake of IGFBP-5, suggesting an interaction between the CSD peptide and IGFBP-5. In other words, IGFBP-5 might be a direct target of Cav-1 or could be an indirect target as a Cav-1-bound protein. In this regard, the consensus sequences of CSD peptide ligands have been identified [40]. The sequences, $\phi X\phi XXXX\phi$, $\phi XXXX\phi XX\phi$, and $\phi X\phi XXXX\phi XX\phi$, where ϕ is any of the aromatic acids (F, W, or Y) and X is any amino acid, are the first described as Cav-1 binding domains responsible for the interaction of Cav-1 with other proteins. Signaling molecules, G-protein receptors, and growth factor receptors, including MAP kinases, eNOS, endothelin R, EGF-R, and IGFBP-3 that are known to be caveolin-associated proteins, contain these motifs [40,41]. Broader consensus Cav-1 binding sequences, in which a hydrophobic amino acid (I, V, or L) replaces aromatic acids in addition to F, W, or Y, were subsequently reported [42]. We speculate that IGFBP-5 might be a direct target of Cav-1 since IGFBP-5 contains the sequence **ICWCVDKY**²⁴⁷, an imperfect consensus sequence with homology to $\phi XZXXXX\phi$ or $ZXXXX\phi XXZ$ where Z stands for F, W, Y, I, V, or L.

Nuclear translocation of IGFBP-3 and IGFBP-5 has been reported in vascular smooth muscle cells, T47D human breast carcinoma cells, and Chinese hamster ovary (CHO) cells [20,24,25]. Since inhibition of protein secretion abolished IGFBP nuclear localization, it was deduced that nuclear IGFBP-3 and -5 are derived from the secreted proteins [20,41]. We have also reported that nuclear translocation of IGFBP-5 occurs in a time-dependent, MAPK-dependent, and IGF-I independent manner [30]. The internalization and nuclear transport of IGFBP-3, a protein with significant homology to IGFBP-5 containing a nuclear localization sequence, is documented in a variety of cells and includes caveolin- and clathrin-dependent pathways [24,25,41]. However, pathways mediating the internalization of IGFBP-5 have not been reported, especially in primary cells such as fibroblasts. Our current study identified the caveolin pathway as a mediator of IGFBP-5 internalization in primary fibroblasts. It is not likely that the caveolin-dependent pathway is the sole mediator of IGFBP-5 uptake, as neither caveolar disruption nor absence of Cav-1 completely inhibited IGFBP-5 uptake. As both caveolin- and transferrin-mediated endocytosis are responsible for IGFBP-3 internalization [41], other pathways, including the transferrin-dependent classical pathway [43] and heparan sulfate proteoglycan-associated internalization [44] may also be involved in IGFBP-5 endocytosis. The latter is likely based on the ability of IGFBP-5 to interact with heparan sulfate proteoglycans [45].

Electron microscopy revealed the presence of cytoplasmic and nuclear aggregates composed mainly of IGFBP-5 in IGFBP-5-expressing fibroblasts. Interestingly, Cav-1 was also detected inside these aggregates, suggesting that they may have originated from the plasma membrane. This suggests a scenario whereby secreted IGFBP-5 was taken up into caveolae, which subsequently formed intracellular vesicle-like structures that trafficked to the nucleus. Our finding is in partial agreement with a recent report showing that IGFBP-5 is found in vesicular structures in T47D cells [37]. However, in this report, IGFBP-5-containing vesicles were not detected in the nucleus. Thus unlike the observations in T47D cells, we clearly show using electron microscopy that IGFBP-5 translocates to the nuclear compartment in inclusions that lack a membrane and are not true vesicles. The fact that IGFBP-5 forms multimers [46] may explain, at least in part, its ability to form aggregates. The differences between our observations and those of Jergeit et al may be attributed to the cell types as they used immortalized cancer cell lines whereas we used primary fibroblasts, or the use of replication-deficient adenovirus to drive the expression of IGFBP-5 in our system. However the latter is unlikely as expression of IGFBP-3 using the same adenoviral construct did not result in the formation of vesicles or aggregates (data not shown). One of the limitations of immuno EM used to confirm the presence of IGFBP-5 and Cav-1 in the nucleus is that detection of proteins is limited to those that are abundant as sections (70 nm) are notably thinner than those use for immunohistochemistry or immunofluorescence staining (6 μ M). Thus, although few 10-nm gold particles identifying Cav-1 were detected, the sheer presence of these particles suggests that Cav-1 is abundant in the nuclei of IGFBP-5-expressing fibroblasts.

Although Cav-1 is a major membrane protein, our data demonstrate that Cav-1 is also localized in the nucleus. Several studies support our findings. For example, VEGF induces nuclear translocation of Flk-1/KDR, eNOS, and Cav-1 in vascular endothelial cells [47]. Increased nuclear localization of Cav-1 was also reported in human diploid fibroblasts in H₂O₂-induced premature senescence [48]. Furthermore, Dittmann *et al* reported that Cav-1 dependent EGF-R internalization was induced by irradiation in a src-dependent manner, and subsequently Cav-1 and EGF-R were shuttled into the nucleus and induced DNA damage [49]. Likewise, Cav-1 mediates the internalization and nuclear compartmentalization of several proteins, and likely has a regulatory function. Thus, the role of nuclear Cav-1, in conjunction with the pro-fibrotic activity of IGFBP-5, is novel and warrants further exploration.

Since it has been reported that IGFBP-5 can interact with several ECM components, including FN, collagen, and proteoglycans [28,45,50], we performed an ECM degradation assay to explore the effects that reduced Cav-1 levels and resulting increased extracellular IGFBP-5 deposition have on the fibrotic phenotype. Our results show that IGFBP-5 bound FN in the ECM and as a result protected FN from proteolytic degradation *in vitro*. Recently, decreased Cav-1 expression in skin and lung fibroblasts of patients with SSc and IPF has been reported [12,13]. Furthermore, we have reported increased IGFBP-5 in fibroblasts, skin, and lung tissues from patients with these same diseases [27,28]. We now show that Cav-1 deficiency results in increased deposition of secreted IGFBP-5 in the ECM and that this IGFBP-5 can bind ECM components and prevent their degradation. Our findings establish a mechanism by which decreased Cav-1 and increased IGFBP-5 in concert promote the progression and perpetuation of fibrosis. We thus propose a scenario where SSc and IPF fibroblasts secrete IGFBP-5 [27,28]. Secreted IGFBP-5 induces production of collagen and fibronectin [29] and accumulates in the ECM due to inefficient internalization in fibrotic cells that have reduced Cav-1 levels [12,13]. IGFBP-5 in the ECM binds components of the ECM and protects them from proteolytic degradation, thus perpetuating the accumulation of ECM components and supporting the fibrotic phenotype. In addition, we recently reported that IGFBP-5 has a chemoattractant activity and promotes the migration of mononuclear

cells into lung tissues[29,30,32] and the transition of fibroblasts and epithelial cells to a myofibroblastic phenotype[29–32]. Both immune cell infiltration and the activation of fibroblasts into myofibroblasts are implicated in the development of fibrosis. Thus, IGFBP-5 contributes to the fibrotic phenotype via promoting the production and deposition of ECM components, protecting ECM components from degradation, the recruitment of mononuclear cells and fibroblasts, and the activation of fibroblasts.

Restoration of Cav-1 function using Cav-1 CSD peptide has been suggested as a potential therapeutic strategy in SSc and IPF patients [16], as Cav-1 inhibits TGF- β signaling by promoting the degradation of the TGF- β receptor and preventing Smad 2 phosphorylation[14]. Systemic administration of Cav-1 CSD peptide to bleomycin-treated mice dramatically inhibited epithelial cell apoptosis, inflammatory cell infiltration, activation of signaling molecules, and expression of ECM components[16]. In our study, treatment with Cav-1 CSD peptide induced rapid uptake of extracellular IGFBP-5, thus reducing extracellular levels of IGFBP-5. Taken together, these findings suggest that administration of Cav-1 CSD peptide may have beneficial effects in fibrosis. However, in contrast to fibroblasts, an increase of Cav-1 expression in endothelial cells was reported during lung fibrogenesis [10]. In addition, pulmonary artery smooth muscle cells (PASMC) from patients with idiopathic pulmonary arterial hypertension (IPAH) have increased Cav-1 levels which contributes to PASMC proliferation and hypertrophy of the pulmonary vascular wall[51], an effect opposite the phenotype described in Cav-1 null mice [17,18]. Thus, as for any potential therapy tested *in vitro* and *in vivo* in animals, a therapeutic approach using CSD peptide should be explored cautiously.

In summary, we show that IGFBP-5 is internalized via caveolin-1-containing lipid rafts and trafficks to the nucleus in vesicular-like inclusions. IGFBP-5 deposition in the ECM is accentuated in Cav-1-deficient lung fibroblasts, promoting the fibrotic phenotype by supporting the accumulation of IGFBP-5 in the extracellular milieu and its binding to components of the ECM, thus preventing their degradation. As decreased expression of Cav-1 in fibroblasts from SSc and IPF patients has been reported [12,13], our findings provide new insights into mechanisms used by IGFBP-5 to induce and promote fibrosis and the role of Cav-1 in the compartmentalization and trafficking of IGFBP-5.

Acknowledgments

This work is supported by a grant AR050840 from the National Institutes of Health. The authors would like to thank Katie Clark and Mara Sullivan for technical assistance with electron microscopy.

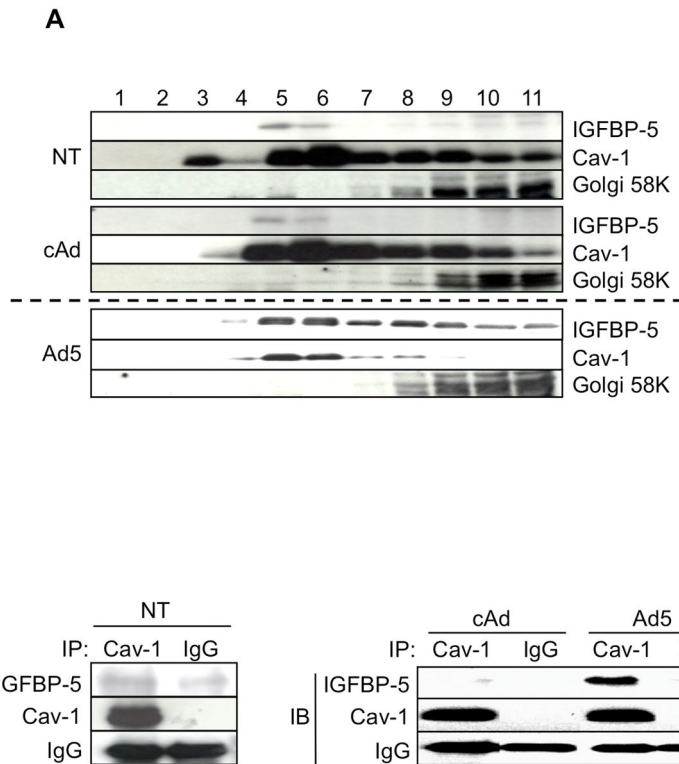
References

1. Steen VD, Medsger TA Jr. Severe organ involvement in systemic sclerosis with diffuse scleroderma. *Arthritis Rheum.* 2000; 43:2437–44. [PubMed: 11083266]
2. Katzenstein AL, Myers JL. Idiopathic pulmonary fibrosis: clinical relevance of pathologic classification. *Am J Respir Crit Care Med.* 1998; 157:1301–15. [PubMed: 9563754]
3. Pardo A, Selman M. Matrix metalloproteases in aberrant fibrotic tissue remodeling. *Proc Am Thorac Soc.* 2006; 3:383–8. [PubMed: 16738205]
4. Liu X, Wu H, Byrne M, Jeffrey J, et al. A targeted mutation at the known collagenase cleavage site in mouse type I collagen impairs tissue remodeling. *J Cell Biol.* 1995; 130:227–37. [PubMed: 7790374]
5. Varga J, Abraham D. Systemic sclerosis: a prototypic multisystem fibrotic disorder. *J Clin Invest.* 2007; 117:557–67. [PubMed: 17332883]
6. Yamada E. The fine structure of the gall bladder epithelium of the mouse. *J Biophys Biochem Cytol.* 1955; 1:445–58. [PubMed: 13263332]

7. Schlegel A, Pestell RG, Lisanti MP. Caveolins in cholesterol trafficking and signal transduction: implications for human disease. *Front Biosci.* 2000; 5:D929–37. [PubMed: 11102315]
8. Parton RG, Richards AA. Lipid rafts and caveolae as portals for endocytosis: new insights and common mechanisms. *Traffic.* 2003; 4:724–38. [PubMed: 14617356]
9. Galbiati F, Razani B, Lisanti MP. Emerging themes in lipid rafts and caveolae. *Cell.* 2001; 106:403–11. [PubMed: 11525727]
10. Kasper M, Reimann T, Hempel U, et al. Loss of caveolin expression in type I pneumocytes as an indicator of subcellular alterations during lung fibrogenesis. *Histochem Cell Biol.* 1998; 109:41–8. [PubMed: 9452954]
11. Tourkina E, Pal Gooz, Pannu J, et al. Opposing effects of protein kinase Ca and protein kinase $\text{C}\epsilon$ on collagen expression by human lung fibroblasts are mediated via MEK/ERK and caveolin-1 signaling. *J Biol Chem.* 2005; 280:13879–87. [PubMed: 15691837]
12. Galdo FD, Sotgia F, de Almeida CJ, et al. Decreased expression of caveolin 1 in patients with systemic sclerosis: Crucial role in the pathogenesis of tissue fibrosis. *Arthritis Rheum.* 2008; 58:2854–65. [PubMed: 18759267]
13. Wang XM, Zhang Y, Kim HP, et al. Caveolin-1: a critical regulator of lung fibrosis in idiopathic pulmonary fibrosis. *J Exp Med.* 2006; 203:2895–906. [PubMed: 17178917]
14. Razani B, Zhang XL, Bitzer M, et al. Caveolin-1 regulates transforming growth factor (TGF)- β /Smad signaling through an interaction with TGF- β type I receptor. *J Biol Chem.* 2001; 276:6727–38. [PubMed: 11102446]
15. Kim S, Lee Y, Seo JE, et al. Caveolin-1 increases basal and TGF- β 1-induced expression of type I procollagen through PI-3 kinase/Akt/mTOR pathway in human dermal fibroblasts. *Cell signal.* 2008; 20:1313–9. [PubMed: 18434090]
16. Tourkina E, Richard M, Gööz P, et al. Antifibrotic properties of caveolin-1 scaffolding domain in vitro and in vivo. *Am J Physiol Lung Cell Mol Physiol.* 2008; 294:L843–61. [PubMed: 18203815]
17. Drab M, Verkade P, Elger M, et al. Loss of caveolae, vascular dysfunction, and pulmonary defects in Caveolin-1 gene-disrupted mice. *Science.* 2001; 293:2449–52. [PubMed: 11498544]
18. Le Lay S, Kurzchalia TV. Getting rid of caveolins: phenotypes of caveolin-deficient animals. *Biochim Biophys Acta.* 2005; 1746:322–33. [PubMed: 16019085]
19. Jones JJ, Clemmons DR. Insulin-like growth factors and their binding proteins: biological actions. *Endocr Rev.* 1995; 16:3–34. [PubMed: 7758431]
20. Xu Q, Li S, Zhao Y, et al. Evidence that IGF binding protein-5 functions as a ligand-independent transcriptional regulator in vascular smooth muscle cells. *Circ Res.* 2004; 94:E46–54. [PubMed: 15001525]
21. Miyakoshi N, Richman C, Kasukawa Y, et al. Evidence that IGF-binding protein-5 functions as a growth factor. *J Clin Invest.* 2001; 107:73–81. [PubMed: 11134182]
22. Andress DL, Loop SM, Zapf J, Kiefer MC. Carboxy-truncated insulin-like growth factor binding protein-5 stimulates mitogenesis in osteoblast-like cells. *Biochem Biophys Res Commun.* 1993; 195:25–30. [PubMed: 7689835]
23. Rajah R, Valentinis B, Cohen P. Insulin-like growth factor (IGF)-binding protein-3 induces apoptosis and mediates the effects of transforming growth factor β -1 on programmed cell death through a p53- and IGF-independent mechanism. *J Biol Chem.* 1997; 272:12181–8. [PubMed: 9115291]
24. Schedlich LJ, Young TF, Firth SM, Baxter RC. Insulin-like growth factor-binding protein (IGFBP)-3 and IGFBP-5 share a common nuclear transport pathway in T47D human breast carcinoma cells. *J Biol Chem.* 1998; 273:18347–52. [PubMed: 9660801]
25. Schedlich LJ, Le Page SL, Firth SM, et al. Nuclear import of insulin-like growth factor-binding protein-3 and -5 is mediated by the importin beta subunit. *J Biol Chem.* 2000; 275:23462–70. [PubMed: 10811646]
26. Andress DL. Insulin-like growth factor-binding protein-5 (IGFBP-5) stimulates phosphorylation of the IGFBP-5 receptor. *Am J Physiol.* 1998; 274:E744–50. [PubMed: 9575837]
27. Feghali CA, Wright T-M. Identification of multiple, differentially expressed messenger RNAs in dermal fibroblasts from patients with systemic sclerosis. *Arthritis Rheum.* 1999; 42:1451–7. [PubMed: 10403273]

28. Pilewski JM, Liu L, Henry AC, et al. Insulin-like growth factor binding proteins 3 and 5 are overexpressed in idiopathic pulmonary fibrosis and contribute to extracellular matrix deposition. *Am J Pathol.* 2005; 166:399–407. [PubMed: 15681824]
29. Yasuoka H, Zhou Z, Pilewski JM, et al. Insulin-like growth factor-binding protein-5 induces pulmonary fibrosis and triggers mononuclear cellular infiltration. *Am J Pathol.* 2006; 169:1633–42. [PubMed: 17071587]
30. Yasuoka H, Hsu E, Ruiz XD, et al. The fibrotic phenotype induced by IGFBP-5 is regulated by MAPK activation and egr-1-dependent and -independent mechanisms. *Am J Pathol.* 2009; 175:605–15. [PubMed: 19628764]
31. Yasuoka H, Jukic DM, Zhou Z, et al. Insulin-like growth factor binding protein 5 induces skin fibrosis: A novel murine model for dermal fibrosis. *Arthritis Rheum.* 2006; 54:3001–10. [PubMed: 16947625]
32. Yasuoka H, Yamaguchi Y, Feghali-Bostwick CA. The pro-fibrotic factor IGFBP-5 induces lung fibroblasts and mononuclear cell migration. *Am J Respir Cell Mol Biol.* 2009; 41:179–88. [PubMed: 19131643]
33. Yasuoka H, Larregina AT, Yamaguchi Y, Feghali-Bostwick CA. Human skin culture as an ex vivo model for assessing the fibrotic effects of insulin-like growth factor binding proteins. *Open Rheumatol J.* 2008; 2:17–22. [PubMed: 19088866]
34. Kim HP, Wang X, Galbiati F, et al. Caveolae compartmentalization of heme oxygenase-1 in endothelial cells. *FASEB J.* 2004; 18:1080–9. [PubMed: 15226268]
35. Stolz DB, Zamora R, Vodovotz Y, et al. Peroxisomal localization of inducible nitric oxide synthase in hepatocytes. *Hepatology.* 2002; 36:81–93. [PubMed: 12085352]
36. Andrews NC, Faller DV. A rapid micropreparation technique for extraction of DNA-binding proteins from limiting numbers of mammalian cells. *Nucleic Acids Res.* 1991; 19:2499. [PubMed: 2041787]
37. Jurgeit A, Berlato C, Obrist P, et al. Insulin-like growth factor-binding protein-5 enters vesicular structures but not the nucleus. *Traffic.* 2007; 8:1815–28. [PubMed: 17892529]
38. Gashler A, Sukhatme VP. Early growth response protein 1 (Egr-1): prototype of a zinc-finger family of transcription factors. *Prog Nucleic Acid Res Mol Biol.* 1995; 50:191–224. [PubMed: 7754034]
39. Okamoto T, Schlegel A, Scherer PE, Lisanti MP. Caveolins, a family of scaffolding proteins for organizing “preassembled signaling complexes” at the plasma membrane. *J Biol Chem.* 1998; 273:5419–22. [PubMed: 9488658]
40. Couet J, Li S, Okamoto T, et al. Identification of peptide and protein ligands for the caveolin-scaffolding domain. Implications for the interaction of caveolin with caveolae-associated proteins. *J Biol Chem.* 1997; 272:6525–33. [PubMed: 9045678]
41. Lee KW, Liu B, Ma L, et al. Cellular internalization of insulin-like growth factor binding protein-3: distinct endocytic pathways facilitate re-uptake and nuclear localization. *J Biol Chem.* 2004; 279:469–76. [PubMed: 14576164]
42. Carman CV, Lisanti MP, Benovic JL. Regulation of G protein-coupled receptor kinases by caveolin. *J Biol Chem.* 1999; 274:8858–64. [PubMed: 10085129]
43. Hopkins CR, Trowbridge IS. Internalization and processing of transferrin and the transferrin receptor in human carcinoma A431 cells. *J Cell Biol.* 1983; 97:508–21. [PubMed: 6309862]
44. Hsia E, Richardson TP, Nugent MA. Nuclear localization of basic fibroblast growth factor is mediated by heparan sulfate proteoglycans through protein kinase C signaling. *J Cell Biochem.* 2003; 88:1214–25. [PubMed: 12647303]
45. Hsieh T, Gordon RE, Clemmons DR, et al. Regulation of vascular smooth muscle cell responses to insulin-like growth factor (IGF)-I by local IGF binding proteins. *J Biol Chem.* 2003; 278:42886–92. [PubMed: 12917428]
46. Koedam JA, Hoogerbrugge CM, Van Buul-Offers SC. Insulin-like growth factor binding protein-3 and -5 form sodium dodecyl sulfate-stable multimers. *Biochem Biophys Res Commun.* 1997; 240:707–14. [PubMed: 9398631]

47. Feng Y, Venema VJ, Venema RC, et al. VEGF induces nuclear translocation of Flk-1/KDR, endothelial nitric oxide synthase, and caveolin-1 in vascular endothelial cells. *Biochem Biophys Res Commun.* 1999; 256:192–7. [PubMed: 10066445]
48. Chrétien A, Piront N, Delaive E, et al. Increased abundance of cytoplasmic and nuclear caveolin 1 in human diploid fibroblasts in H₂O₂-induced premature senescence and interplay with p38alpha(MAPK). *FEBS Lett.* 2008; 582:1685–92. [PubMed: 18439424]
49. Dittmann K, Mayer C, Kehlbach R, Rodemann HP. Radiation-induced caveolin-1 associated EGFR internalization is linked with nuclear EGFR transport and activation of DNA-PK. *Mol Cancer.* 2008; 7:69. [PubMed: 18789131]
50. Jones JI, Gockerman A, Busby WH Jr, et al. Extracellular matrix contains insulin-like growth factor binding protein-5: potentiation of the effects of IGF-I. *J Cell Biol.* 1993; 121:679–87. [PubMed: 7683690]
51. Patel HH, Zhang S, Murray F, et al. Increased smooth muscle cell expression of caveolin-1 and caveolae contribute to the pathophysiology of idiopathic pulmonary arterial hypertension. *FASEB J.* 2007; 21:2970–9. [PubMed: 17470567]

**Figure 1.**

The localization and binding of Cav-1 and IGFBP-5. **A:** Caveolae-enriched membrane fractionation was analyzed by immunoblotting for IGFBP-5 and Cav-1. Twelve fractions were obtained from human lung fibroblasts that were infected with cAd, Ad5, or untreated (NT) for 48h using sucrose density gradient fractionation. Eleven fractions (fractions 1–11) were subjected to western blot analysis for IGFBP-5, Cav-1, and 58k Golgi protein as a control for the fractionation. Different exposure times for NT, cAd, and Ad5 are shown as the levels of IGFBP-5 in Ad5 samples were high and the signal was easily saturated. **B:** Protein-protein interaction between IGFBP-5 and Cav-1 was examined by immunoprecipitation using anti-Cav-1 antibody. Primary lung fibroblasts were non-treated or infected with Ad5 or cAd at an MOI of 50 and cellular lysates were harvested 72 hours post-treatment. Lysates were immunoprecipitated (IP) with anti-Cav-1 antibody or rabbit IgG (IgG). Co-precipitation of IGFBP-5 was examined by immunoblotting (IB). Cav-1 and rabbit immunoglobulins are shown as controls. Left panel; Non-treated cells (NT). Right panel; cAd-or Ad5-infected cells.

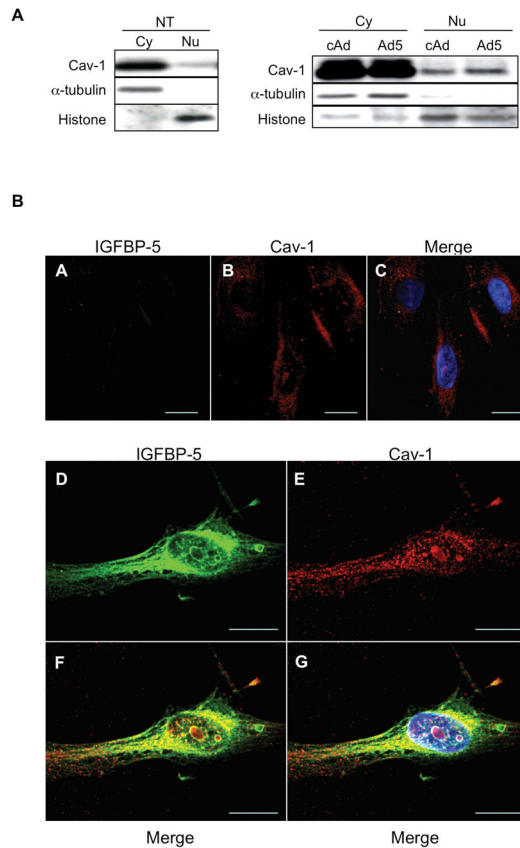


Figure 2. Nuclear translocation of Cav-1 in IGFBP-5-expressing fibroblasts. **A:** 1×10^6 human lung fibroblasts were cultured on 100mm dishes and untreated or infected with cAd or Ad5 at an MOI of 50. After 24h, cytoplasmic and nuclear extracts were prepared and expression of Cav-1 was examined by western blot. Cytoplasmic extracts from 5×10^4 cell-equivalent or nuclear extracts from 1×10^5 cell-equivalent was applied to each lane. Alpha-tubulin is shown as a loading control for cytoplasmic extracts, and histone for nuclear extracts. Left panel; Non-treated cells (NT). Right panel; cAd- or Ad5-infected cells. **B:** Expression of IGFBP-5 and Cav-1 was examined by immunofluorescence. Human lung fibroblasts were cultured on cover slips coated with type I collagen. After infection using cAd (**A–C**) or Ad5 (**D–G**) for 48h, cells were stained for IGFBP-5 (green) and Cav-1 (red). Hoechst (blue) was used to identify nuclei. Magnification of images ranged from 800x to 1000x on a confocal microscope. Scale bars = 20 μ m.

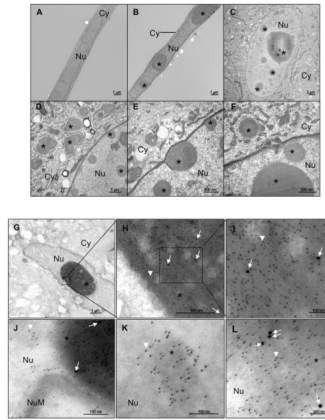


Figure 3. Detection of IGFBP-5 and Cav-1 in nuclei by electron microscopy (EM). **A–F:** Human lung fibroblasts were infected with cAd (**A**) or Ad5 (**B–F**) for 48 h, fixed, and analyzed by transmission electron microscopy. Cy: cytoplasm; Nu: nucleus; *: aggregates. **G–L:** Ad5-infected human fibroblasts subjected to immuno-TEM. **H** and **I** represent magnified regions of the nucleus shown in **G**. **J–L** show higher magnification of gold particles detected in inclusions and protein aggregates in the nucleus. Ten nm gold particles (white arrow) identify Cav-1, and 5 nm gold particles (representative white arrowheads) identify IGFBP-5. Size of bars is indicated.

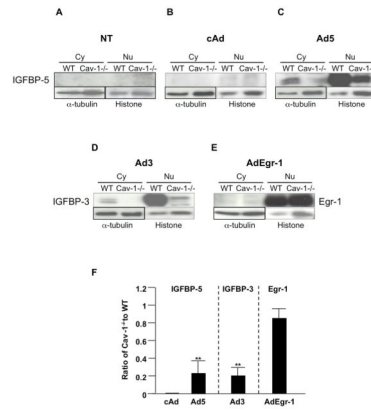


Figure 4.

IGFBP-5 (A–C), IGFBP-3 (D), and Egr-1 (E) levels in cytoplasmic and nuclear extracts from WT and Cav-1^{-/-} fibroblasts. Cytoplasmic and nuclear fractions were extracted from WT and Cav-1^{-/-} fibroblasts that were untreated or infected with the indicated adenoviral constructs for 48 h. Cytoplasmic and nuclear extracts were subjected to immunoblotting for the detection of IGFBP-5, IGFBP-3, and Egr-1. Alpha-tubulin is shown as a loading control for cytoplasmic extracts, and histone for nuclear extracts. F: Graphical summary of data is shown in panels B–E. The signal intensity of each protein in nuclear extracts was normalized to histone, and the ratio of the intensity in Cav-1^{-/-} to WT was calculated. Differences in levels between WT and Cav-1^{-/-} cells were compared using the unpaired *t*-test. Horizontal bars indicate mean values of 2 independent experiments. ** *P* < 0.01.

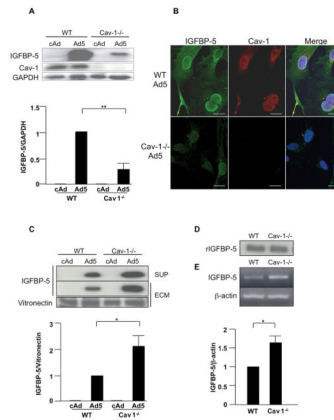
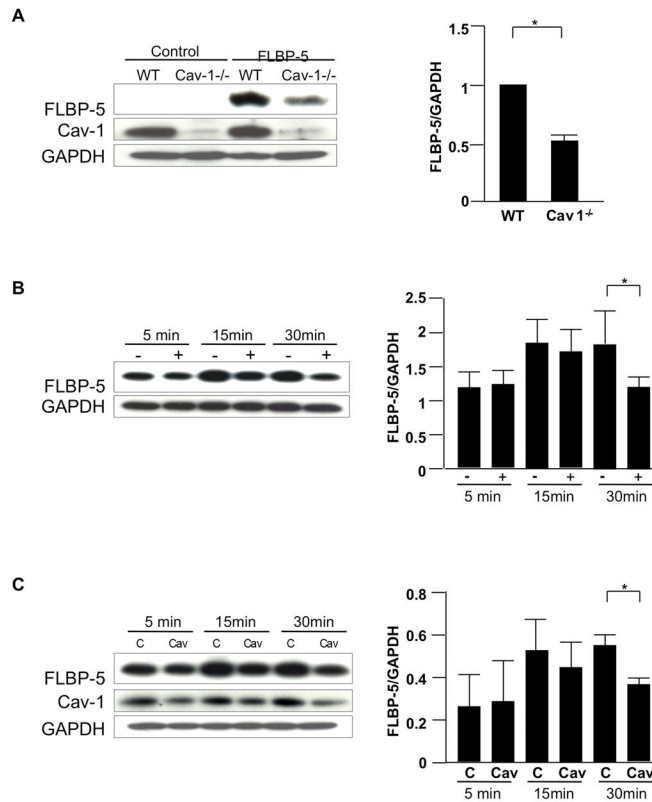


Figure 5.

IGFBP-5 levels in lysates, supernatants, and ECM of WT and Cav-1^{-/-} lung fibroblasts. Cultured WT and Cav-1^{-/-} fibroblasts were infected with cAd and Ad5 at an MOI of 50. Lysates, supernatants, and ECM were harvested after 48 h (A) or 72h (C). Levels of IGFBP-5 were analyzed by immunoblotting of lysates (A), supernatants (SUP) and ECM (C). GAPDH and vitronectin were used as loading controls for lysates and ECM, respectively. For the supernatant, an equivalent amount of total protein was loaded in each lane. Graphical summary of IGFBP-5 expression in lysates (A) and ECM (C) from WT and Cav-1^{-/-} fibroblasts. The unpaired *t*-test was used for statistical analysis. Horizontal bars indicate mean values of 3 independent experiments for (A) and 2 independent experiments for (C). * *P* < 0.05, ** *P* < 0.01. **B:** IGFBP-5 and Cav-1 localization was examined by immunocytostaining. WT and Cav-1^{-/-} fibroblasts were cultured on cover slips coated with type I collagen. After infection with Ad5 for 48h, cells were stained for IGFBP-5 (green) and Cav-1 (red). Hoechst (blue) was used to identify nuclei. Magnification of images was 600x on a confocal microscope. Scale bars = 20 μ m. **D:** western blot analysis of rIGFBP5 levels following a 1 h incubation with media conditioned by WT and Cav-1^{-/-} fibroblasts. **E:** Steady-state mRNA levels of mouse IGFBP-5 in non-treated WT and Cav-1^{-/-} fibroblasts. β -actin was used as a control. Normalized IGFBP-5 mRNA levels in WT were arbitrarily set at 1. Horizontal bars indicate mean values of 3 independent experiments. The unpaired *t*-test was used for statistical analysis.

**Figure 6.**

Internalization of IGFBP-5. **A:** WT and Cav-1^{-/-} fibroblasts were plated at 70% confluence in serum-free media. FLAG-tagged IGFBP-5 (FLBP-5) was added to each well. After 15 minutes, lysates were harvested and subjected to western blot analysis. IGFBP-5 in lysates from WT and Cav-1^{-/-} fibroblasts was detected using anti-FLAG M2 antibody. GAPDH was used as a loading control. Normalized FLBP-5 levels in WT fibroblasts were arbitrarily set at 1. Horizontal bars indicate mean values of 2 independent experiments. The unpaired *t*-test was used for statistical analysis. * $P < 0.05$. **B:** WT fibroblasts were cultured with (+) or without (-) 10mM M β CD for 1h in serum-free media, and FLBP-5 was added to each well. After 5, 15, and 30 minutes, lysates were harvested and subjected to western blot analysis. IGFBP-5 in lysates was detected using anti-FLAG M2 antibody. GAPDH was used as a loading control. Horizontal bars indicate mean values of 3 independent experiments. Data were analyzed using the paired *t*-test. * $P < 0.05$. **C:** WT fibroblasts were transfected with control scrambled siRNA (C) or siCav-1 (Cav) for 48h, and then FLBP-5 was added to each well. After 5, 15, and 30 minutes, lysates were harvested and subjected to western blot analysis. IGFBP-5 in lysates was detected using anti-FLAG M2 antibody. GAPDH was used as a loading control. Horizontal bars indicate mean values of 3 independent experiments. Data were analyzed using the paired *t*-test. * $P < 0.05$.

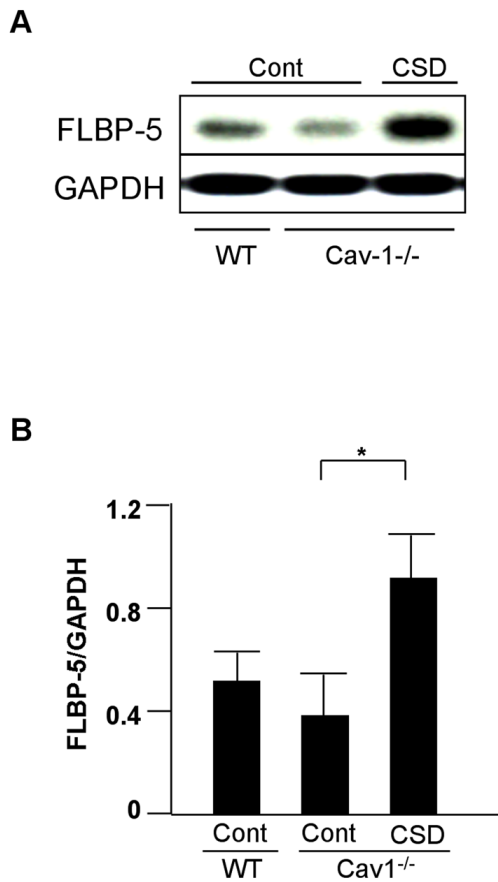
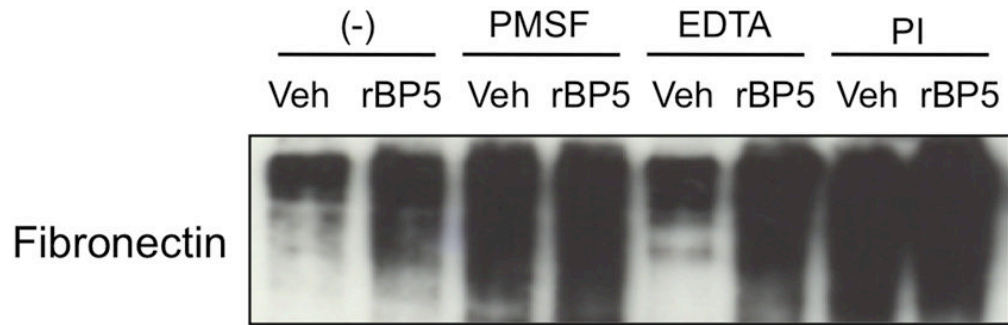


Figure 7. IGFBP-5 uptake following restoration of Cav-1 function. **A:** WT or Cav-1^{-/-} fibroblasts were treated with Cav-1 CSD peptide (CSD) or control peptide (Cont) for 1h in serum-free medium, then FLAG-tagged IGFBP-5 (FLBP-5) was added. After 15 minutes, lysates were harvested and subjected to western blot analysis. IGFBP-5 levels in lysates were detected using anti-FLAG M2 antibody. GAPDH was used as a loading control. **B:** Graphical analysis of IGFBP-5 levels in lysates of WT and Cav-1^{-/-} fibroblasts following 1h incubation with Cav-1 CSD (CSD) or control peptide (Cont). Horizontal bars indicate mean values from 4 independent experiments. The paired *t*-test was used for statistical analysis. * $P < 0.05$.

**Figure 8.**

ECM degradation assay. Cell culture wells were coated with human plasma fibronectin. Recombinant IGFBP-5 (rBP5) or vehicle (Veh; 10mM HCL) was added for an additional 16h. Medium conditioned by primary fibroblasts was added to the wells in the presence or absence of the protease inhibitors PMSF, EDTA, and PI (protease inhibitor cocktail). After 48h, ECM was harvested and subjected to western blot analysis.